Journal of Marine Research, 42, 29–43, 1984

Double Kelvin waves in a two-layer sea

by S. A. W. Bondok[1] and H. G. Pinsent[2]

ABSTRACT

It is shown that a depth change such as a fault line acts as a wave guide to long period waves in a two-layer rotating sea, in a similar way to the Double Kelvin waves of Longuet-Higgins (1968a, b) for a homogeneous sea. For a sea with a step discontinuity in depth, the effect of an extra layer leads to only small changes in the dispersion characteristics.

For a continuous monotonic depth change taking place over a width l it is found that as l increases the Double Kelvin wave period increases, and the elevation at the interface decreases relative to the free surface elevation.

Finally the effect of a time periodic wind stress suddenly applied is considered for step discontinuity in depth. For a maximum wind stress of 1 dyne the free surface wave amplitudes of the Double Kelvin wave are significantly less than those given by Mysak (1968). The corresponding interface amplitudes are about 10 cm. It is suggested, unlike their one-layer counterparts, that it may be possible to detect the two-layer waves successfully in practice, since they are predicted to have relatively large elevations at the interface.

1. Introduction

Energy can be propagated freely in the form of plane long waves across a sea of constant depth, and constant Coriolis parameter f, provided the wave frequency $\sigma > f$. If there is no restriction on the frequency, wave energy can in fact be propagated long distances, but only around coastlines bounding the sea in the form of Kelvin waves. In these waves the amplitude decays exponentially with distance away from the coast.

Longuet-Higgins (1968a, b) has shown that in theory energy can be similarly guided across a homogeneous one-layer sea provided a change of depth exists; for example, a geological fault line. He called this wave a Double Kelvin wave. Mysak (1968) deals with the generation of Double Kelvin waves. In these waves, which as far as we know are still undetected in practice, the wave amplitude is predicted to decay exponentially with distance on each side of the change in depth. For these waves $f > \sigma$, if the depth changes are monotonic, and such waves could be significant in transferring energy across open sea when plane waves are not available to do so. In this discussion we are of course excluding β-plane waves which only apply on an ocean scale and have very long

1. Al-Azhar University, Egypt.
2. Department of Mathematics, Chelsea College, University of London, 552 King's Road, London, England, SW10 OUA.

periods. In the present paper we wish to extend Longuet-Higgins' work to consider a sea with two density layers as a more realistic approximation to a sea with a thermocline. There is an important practical reason for such an extension which we now develop.

For a two-layer sea, two completely independent plane wave modes are possible for $\sigma > f$, an ordinary wave which is identical to that found in a one-layer sea, and an internal wave which displays amplitude changes at the density interface about 30 times larger than those occurring at the free surface. If the depth is variable these plane waves lose their separate identity and display both ordinary and internal wave characteristics. Waves with exponential decay behavior are similar in many respects to plane waves. It seems reasonable, therefore, to infer that if a Double Kelvin wave exists in a two-layer sea having a depth change, it must also display dual characteristics. This then implies that it may be possible to detect a Double Kelvin wave in practice by observations in the vicinity of the thermocline, where the interface elevations could be expected to be large due to internal effects. By the same reasoning, purely homogeneous Double Kelvin waves would not appear to be possible in a sea with a strongly developed thermocline.

Basic equations. We take a two-layer sea consisting, when undisturbed, of an upper layer of density ρ and thickness h, over a lower layer of density $\rho' = \rho/\gamma$, where $\gamma < 1$, see Figure 1. We take coordinates (x, y, z) with z vertically upward. The bottom of the sea is variable and given by $z = -H(x)$. If ζ, ζ' are the surface and the interface elevations caused by the wave motion, the hydrostatic pressure distribution is

$$p = p_a + \rho g(\zeta - z), \tag{1}$$

$$p = p_a + \rho g(\zeta + h - \zeta') + \rho' g(\zeta' - h - z), \tag{2}$$

where p_a is the atmospheric pressure, g acceleration due to gravity, and the prime refers, as always here, to the lower layer.

Substituting for the pressure in the equations of horizontal motion, ignoring vertical velocities compared to horizontal ones (u, v) and (u', v') in the (x, y) directions, then we have at time t,

$$u_t - fv = -g\zeta_x + \tau^x/\rho h, \qquad v_t + fu = -g\zeta_y + \tau^y/\rho h, \tag{3}$$

$$u'_t - fv' = -gM_x, \qquad v'_t + fu' = -gM_y, \tag{4}$$

where

$$M = \gamma\zeta + (1 - \gamma)\zeta', \tag{5}$$

and (τ^x, τ^y) is the wind stress at the free surface of the ocean. We have ignored stresses at the interface and at the sea bottom. The corresponding continuity equations are

$$h(u_x + v_y) = -(\zeta - \zeta')_t. \tag{6}$$

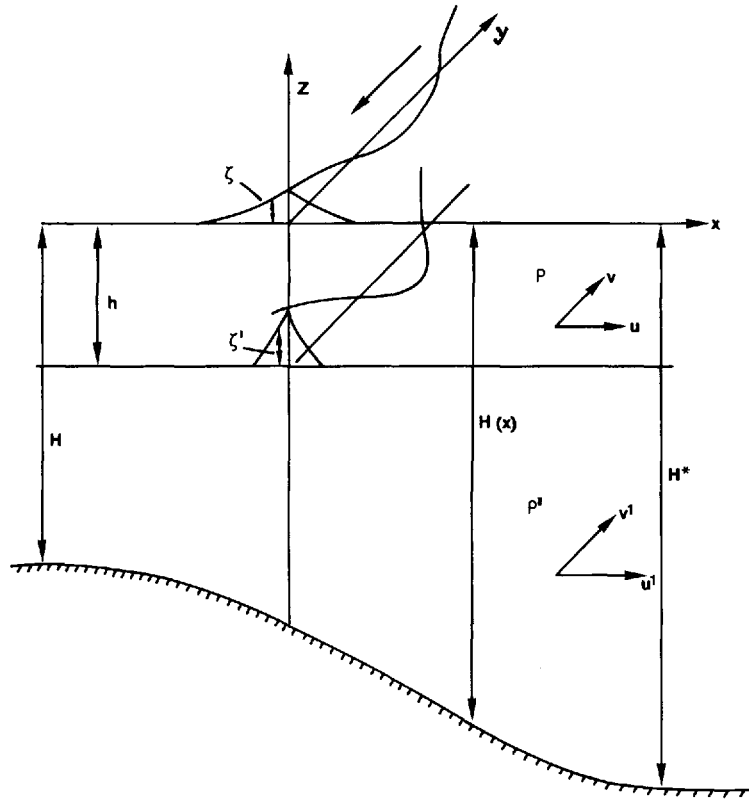

Figure 1. Guided waves being propagated along the transition zone between two regions of uniform depth for a two-layer ocean.

and

$$[(H(x) - h)u']_x + (H(x) - h)v'_y = -\zeta'_t. \tag{7}$$

In the first part of this paper we are particularly interested in the existence of guided waves propagating parallel to the lines of constant depth in the y direction. We will therefore ignore the wind stresses until the final section and assume all perturbed quantities have a $e^{imy - i\sigma t}$ dependence where m is a wavenumber. For simplicity we retain the same notation for the perturbations, but now it is understood they all depend only on x. From (3), (4) we obtain the velocity perturbations

$$u = -\frac{g}{\sigma^2 - f^2}(i\sigma\zeta_x - ifm\zeta), \qquad v = -\frac{g}{\sigma^2 - f^2}(f\zeta_x - \sigma m\zeta), \tag{8}$$

$$u' = -\frac{g}{\sigma^2 - f^2}(i\sigma M_x - ifm M), \quad v' = -\frac{g}{\sigma^2 - f^2}(fM_x - \sigma m M). \tag{9}$$

Eliminating these using (6) and (7) gives

$$\zeta' = \zeta + \frac{hg}{\sigma^2 - f^2}(\zeta_{xx} - m^2\zeta), \tag{10}$$

$$\zeta' = -\frac{g}{\sigma^2 - f^2} \cdot \left\{\left[(H(x) - g)\left(M_x - \frac{f}{\sigma}mM\right)\right]_x + (H(x) - h)\left(\frac{f}{\sigma}M_x - mM\right)m\right\}. \tag{11}$$

Finally substituting for ζ' from (10) into (11) using (5) gives a fourth order ordinary differential equation for the free stream elevation $\zeta(x)$ i.e.,

$$\left[(1-\gamma)(H(x)-h)(D^2-m^2)^2 - H(x)\frac{f^2-\sigma^2}{gh}(D^2-m^2) + h\left(\frac{f^2-\sigma^2}{gh}\right)^2 + \frac{dH}{dx}\left(D - m\frac{f}{\sigma}\right)\left((1-\gamma)(D^2-m^2) - \frac{f^2-\sigma^2}{gh}\right)\right]\zeta(x) = 0 \tag{12}$$

where D is the differential operator $D = d/dx$.

2. Depth discontinuity

In this case we assume $H(x) = H$ for $x < 0$, and $H(x) = H^*$ for $x > 0$, taking the bottom to be a step of height $H^* - H > 0$ at $x = 0$. For $x < 0$ we look for exponential solutions of the form $e^{nx} \to 0$ as $x \to -\infty$, for constant $n > 0$. (12) yields for $x < 0$,

$$(1-\gamma)(H-h)(n^2-m^2) - H\frac{f^2-\sigma^2}{gh}(n^2-m^2)^2 + h\left(\frac{f^2-\sigma^2}{gh}\right)^2 = 0. \tag{13}$$

For $1 - \gamma \ll 1$, (13) yields two values of n, n_o for an ordinary wave type, and n_i for a wave type with internal characteristics, i.e.

$$n_o^2 = m^2 - \frac{\sigma^2 - f^2}{gH}, \qquad n_i^2 = m^2 - \frac{\sigma^2 - f^2}{(1-\gamma)gh}\frac{H}{(H-h)}. \tag{14}$$

Taking a linear combination of these solutions in terms of constants A_o, A_i and using (8), (9), (10) gives for $x < 0$

$$\zeta = A_o e^{n_o x} + A_i e^{n_i x},$$

$$\zeta' = \left(1 - \frac{h}{H}\right)A_o e^{n_o x} + \left(1 - \frac{H}{(1-\gamma)(H-h)}\right)A_i e^{n_i x},$$

$$u = \frac{gi}{f^2 - \sigma^2}\{(\sigma n_o - fm)A_o e^{n_o x} + (\sigma n_i - fm)A_i e^{n_i x}\},$$

$$u' = \frac{gi}{f^2 - \sigma^2} \cdot \left\{ \left(1 - (1-\gamma)\frac{h}{H} \right) (\sigma n_o - fm) A_o e^{n_o x} - \frac{h}{H-h} (\sigma n_i - fm) A_i e^{n_i x} \right\}. \quad (15)$$

In a similar manner for $x > 0$, results corresponding to (14) and (15) can be obtained replacing A_o, A_i, H, n_o, n_i by $A_o^*, A_i^*, H^*, -n_o^*, -n_i^*$ where $n_o^*, n_i^* > 0$.

The solution may now be completed by matching these results at $x = 0$ using four boundary conditions. By inference from the one layer case of Longuet-Higgins we assume at $x = 0$

$$\zeta = \zeta^*, \; hu = hu^*$$
$$\zeta' = \zeta'^*, \; (H-h)u' = (H^*-h)u'^*, \quad (16)$$

i.e., continuity of free surface and interface elevations, and continuity in each density layer of the total mass flux perpendicular to the step. The conditions (16) give

$$A_o + A_i = A_o^* + A_i^*,$$
$$\left(1 - \frac{h}{H}\right) A_o + \left(1 - \frac{H}{(1-\gamma)(H-h)}\right) A_i = \left(1 - \frac{h}{H^*}\right) A_o^* + \left(1 - \frac{H^*}{(1-\gamma)(H^*-h)}\right) A_i^*$$
$$(\sigma n_o - fm) A_o + (\sigma n_i - fm) A_i = (-\sigma n_o^* - fm) A_o^* + (-\sigma n_i^* - fm) A_i^*,$$
$$(H-h)\left[(\sigma n_o - fm)\left(1 - (1-\gamma)\frac{h}{H}\right) A_o - (\sigma n_i - fm)\frac{h}{H-h} A_i \right] = (H^*-h)\left[(-\sigma n_o^* - fm)\left(1 - (1-\gamma)\frac{h}{H^*}\right) A_o^* + (\sigma n_i^* + fm)\frac{h}{H^*-h} A_i^* \right]. \quad (17)$$

To obtain a consistent solution the fourth order determinant of the unknown constants A_o, A_i, A_o^*, A_i^* must vanish. This leads us directly to a nondimensional equation of the form

$$D(\tau, \epsilon, \bar{h}, \Gamma, \gamma) = 0 \quad (18)$$

where $\tau = -f/\sigma$, $\epsilon = f^2/gH^*m^2$, $\bar{h} = h/H$, and $\Gamma = H^*/H$.

Calculation reveals that these Double Kelvin waves do exist theoretically. In Figure 2 the period measured in pendulum days is shown as a function of ϵ the wavenumber parameter, for various values of $\Gamma(>1)$ and $\bar{h} = 0.5, .5, .95$ in the case $\gamma = \rho/\rho' = .998$. We note that only positive values of τ exist showing that in the Northern Hemisphere ($f > 0$) the wave propagates in the negative y direction with deeper water on the left of

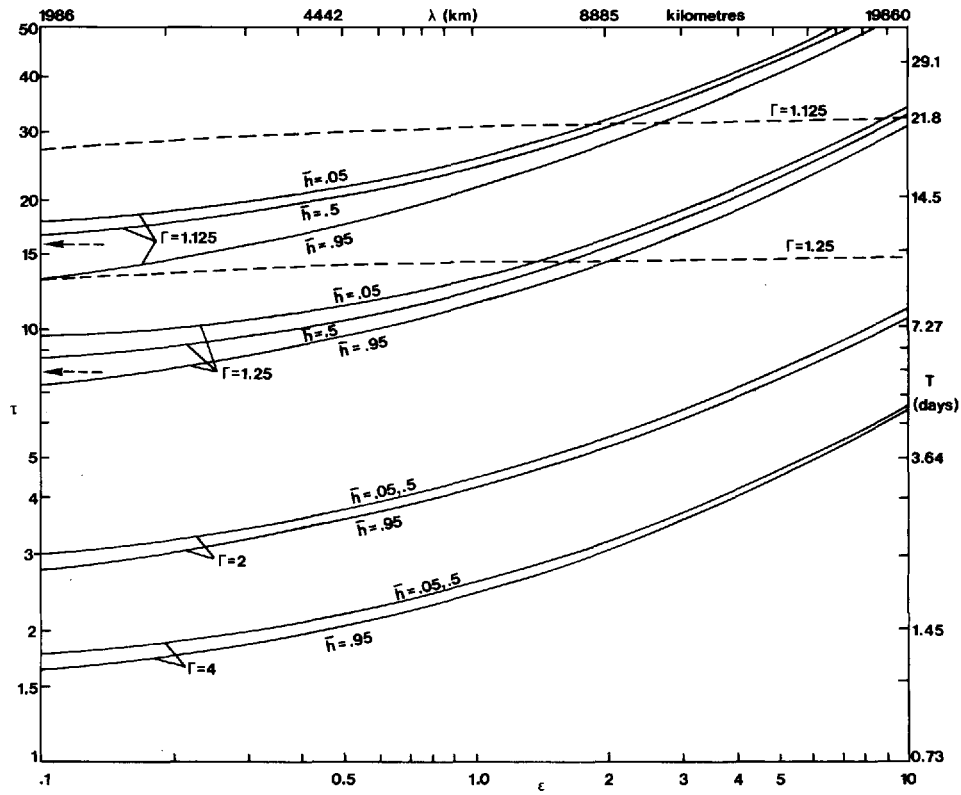

Figure 2. Wave period τ measured in pendulum days against $\epsilon = f^2/m^2gH^*$ for various values of $\Gamma = H^*/H$ and $\bar{h} = h/H$ when $\rho/\rho' = .998$. Also shown are wavelength l and period scales T for the special case $f = 10^{-4}$ sec^{-1}, $H^* = 10^8$ cm, $g = 1000$ cm sec^{-2}. Dashed lines are from (19).

the direction of propagation. In the Southern Hemisphere ($f < 0$) the deep water will lie on the right of the propagation in the positive y direction. In addition we see that $\tau > 1$, i.e., the period of the waves is always greater than a pendulum day. Longuet-Higgins (1968a) puts forward similar conclusions for a homogeneous sea. The results for the case $\bar{h} = 0.05$ in Figure 2 are almost identical to those of the one-layer case which can be shown theoretically from (17) to coincide with the limit $\bar{h} = 0$ as the top layer becomes vanishingly thin. Thus it would appear from Figure 2 that whether the sea is of one or two layers Double Kelvin waves have very similar dispersion relations, and similar properties for the wave lengths, periods and phase velocities.

Rhines (1977), page 275, gives a dispersion relation for a two-layer ocean whose free surface is assumed to be a rigid lid. In our notation this result becomes

$$\tau = 2\left(\frac{\Gamma + 1}{\Gamma - 1}\right)\left(\Gamma + \left(1 + \frac{\epsilon(1 + \Gamma)}{1 - \gamma}\right)^{-1/2}\right)^{-1} \tag{19}$$

being valid for small step changes and therefore Γ values near unity. The results for $\Gamma = 1.125$ and 1.25 are shown as dashed lines on Figure 2.

Also shown are the limiting cases as $\epsilon = f^2/gH^*m^2 \to 0$, given by $\tau = 2/(\Gamma - 1)$. As can be seen from Figure 2 taking free surface effects fully into account does lead to significant differences except in the limiting case $\epsilon \to 0$. These differences will be even more marked in the group velocities $d\sigma/dm$ than in phase velocities σ/m. It would appear from Figure 2 that Longuet-Higgins' one-layer theory with its unrestrained free surface gives more realistic information even for a two-layer ocean than the 'rigid lid' result (19).

Although the one- and two-layer Double Kelvin waves have similar propagation characteristics, they display differences particularly in regions just above the discontinuity. Above $x = 0$ the ratio of maximum interface to free surface elevations, say R, can be quite large. For example for the case $\Gamma = 1.25$, $\tau = 11$, then $R = 70$ if $\bar{h} = 0.5$, $\epsilon = 0.56$, dropping monotonically to $R = 50$ for $\bar{h} = 0.05$, $\epsilon = 0.4$. In the former case if $H^* = 1$ km it can be shown that $R > 10$ for a region of width 80 km above $x = 0$. This yields quite a wide lateral region in which to observe the interface for the possible detection of these waves. Further evidence in this connection is illustrated in the next section (Figs. 5, 6, 7) where we display typical elevation profiles over depth profiles of differing width.

3. Continuous depth case

We follow Longuet-Higgins (1968b), using an identical bottom profile of thickness l defined in our notation as

$$H(x) = \frac{(H + H^*)}{2}\left\{1 + \frac{H^* - H}{H^* + H}\tanh\,(1.83x/l)\right\} \tag{20}$$

where for $|x| < l$, $H(x)$ varies over 95% of its range. For large $|x|$, the solution of (12) will involve a combination of the four solutions described in the last section, two for $x \to +\infty$, and two for $x \to -\infty$. For each solution in turn initial values of ζ and its first three derivatives are found and numerical integration of (12) is carried out using (20) in the transition zone until $x = 0$ is reached. At this point the linear combination of the solutions can be matched by imposing four continuity conditions, i.e., continuity of ζ and its first three derivatives with respect to x. This leads, as in the discontinuous case above, to a fourth order determinant in the form of a Wronskian which must then vanish for consistency.

In Figures 3, 4 we show the periods of the first mode Double Kelvin waves as they vary with the width of the bottom profile for certain values of $\epsilon = f^2/gH^*m^2$, for the two cases $\Gamma = 2$, 1.25 respectively. Results are given also in terms of the nondimensional parameter $L = lf/(gH^*)^{1/2}$ as well as for the actual width l for the special case of $f = 10^{-4}$ sec^{-1}, $g = 1000$ cm sec^{-2}, $H^* = 10^8$ cm. The actual wavelengths are also shown. Higher modes are ignored since they will have much larger periods. The results

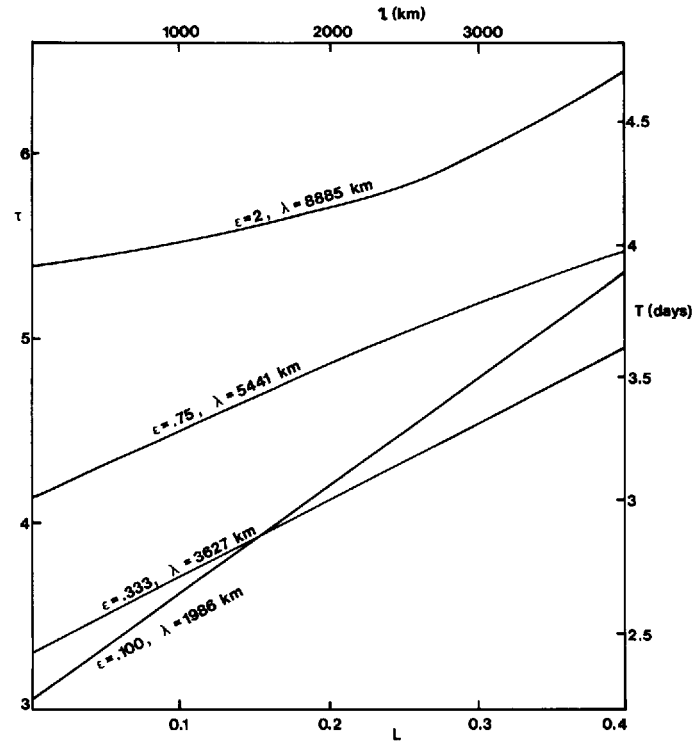

Figure 3. Wave period τ variation against $L = lf/\sqrt{gh}$, where l is the width of depth change for various values of $\epsilon = f^2/gH^*m^2$ for $\Gamma = H^*/H = 2$ and $\rho/\rho' = .998$. Also shown are values of l and wavelengths for the special case $f = 10^{-4}$ sec^7, $H^* = 10^8$ cm, $g = 1000$ cm sec^{-2}.

reduce to those values given in Figure 2 for the limiting case of $l = 0$ for the step discontinuity. As reported by Longuet-Higgins for a homogeneous sea, as the width l, increases the periods of the waves increase, tending eventually to steady motions.

Figures 5, 6, 7 show the unnormalized elevations of the surface and the interface which result from solving Eq. (12) for $L = .025, .26, .42$ respectively for the case $\Gamma = 2$. As in the corresponding one-layer case there is a reduction in elevations as L increases. A significant feature of these results is the way in which the ratio of maximum elevations R reduces from $R = 20$ for $L = .025$, to $R = 4$ for $L = .42$. In addition we observe that the maximum elevations are all shifted toward the shallower end of the depth case. A similar behavior was found by Longuet-Higgins. The Double Kelvin waves do not appear to suffer inversion of the interface elevation relative to the free surface as they are guided along the depth change. This demonstrates that they are not purely baroclinic waves. Two-layer internal plane waves do of course display inverted elevations when they propagate.

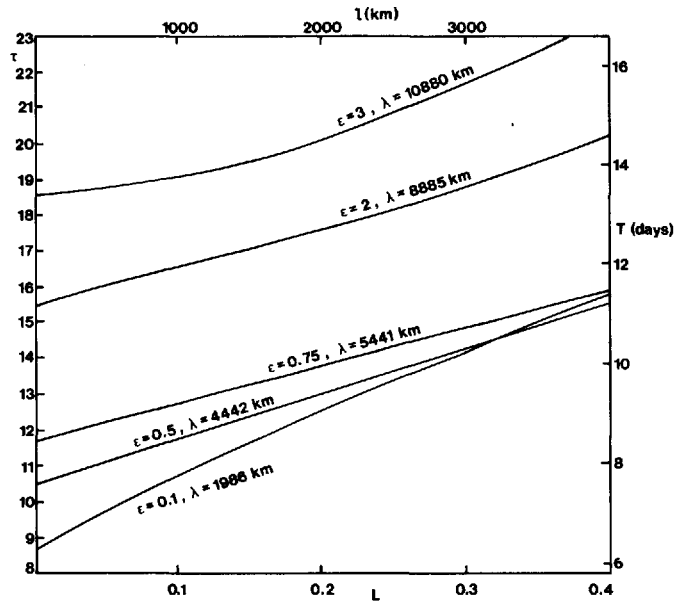

Figure 4. Legend as in Figure 3 but with $\Gamma = H^*/H = 1.25$.

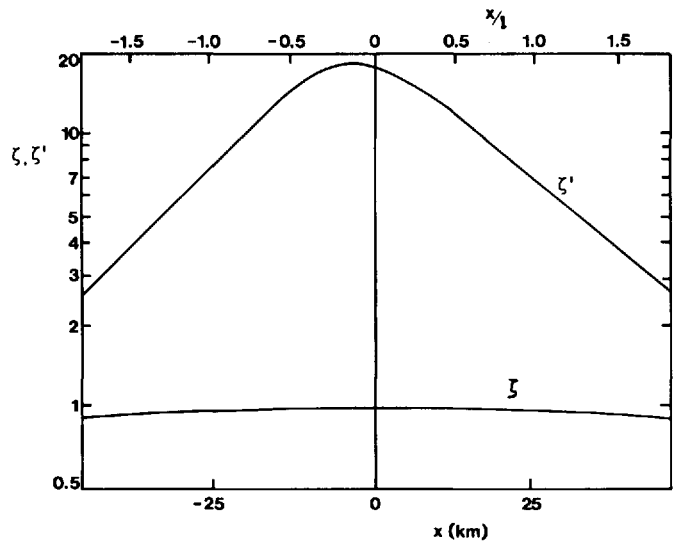

Figure 5. Unnormalized free surface elevation ζ and interface elevation ζ' against x/l and x scales across a continuous depth change of width $l = 25$ km given by (20) for $\rho/\rho' = .998$.

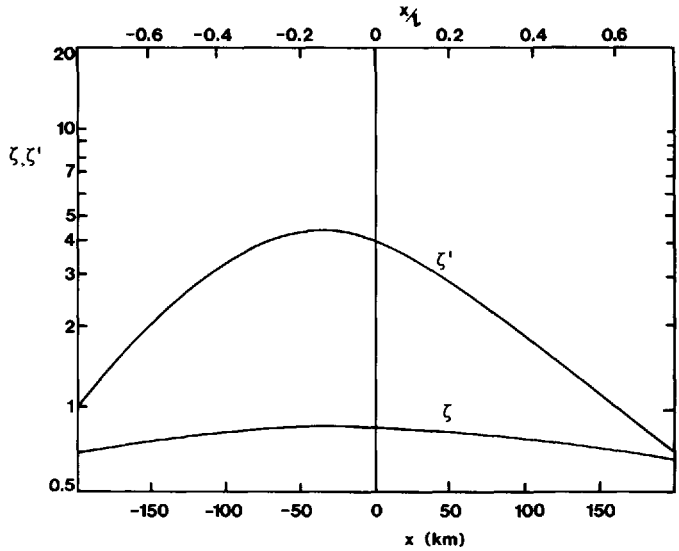

Figure 6. Legend as in Figure 5 but with l = 260 km.

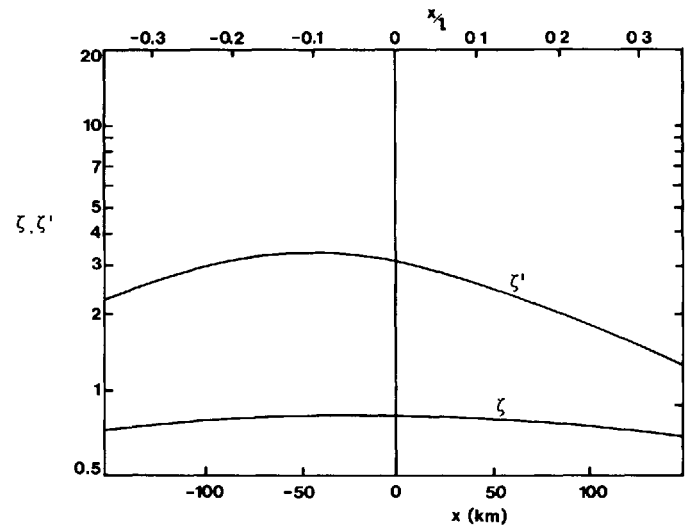

Figure 7. Legend as in Figure 5 but with l = 420 km.

4. Wave generation by wind stress

a. One-layer case. For a one-layer ocean Mysak considers the response to a time periodic wind stress starting up at $t = 0$ of the form

$$\begin{aligned} \tau^x &= \frac{1}{2}\tau_o{}^x H(t) \cos \sigma t \exp(-k|y|), \\ \tau^y &= 0 \text{ where } H(t) = 1 \text{ for } t \geq 0. \\ &\qquad = 0 \text{ for } t < 0. \end{aligned} \tag{21}$$

Mysak points out that this stress field could be regarded as a rough approximation to fluctuating winds caused by alternating anticyclonic and cyclonic weather systems. Concentrating on the region of maximum disturbances directly over a step discontinuity at $x = 0$, Mysak gives the elevation response as a Fourier integral which in our notation becomes the real part of the result:

$$\zeta = -\frac{\tau_o{}^x}{\rho g H^* k}\left\{ e^{i\sigma t}\int_G \frac{B(\alpha)}{K_2{}^2}\left[i - \frac{\alpha(\Gamma-1)}{K_1 E}\left(K_1 - \frac{\alpha}{\tau}\right)\right] \exp(iky\alpha)\, d\alpha \right.$$
$$\left. + \int_G \frac{B(\alpha)\,\Gamma(K_1+K_2)}{\tau E K_1 K_2} \exp(i[ky\alpha + \omega\sigma t])\, d\alpha \right\}, \tag{22}$$

where

$$B(\alpha) = \frac{\alpha\tau}{2\pi(\alpha^2+1)}, \quad E(\alpha) = \alpha(\Gamma-1) + \frac{1}{\tau}(K_1 + \Gamma K_2),$$
$$\omega(\beta) = \frac{(1-\Gamma)\alpha\tau}{(K_1+K_2)}, \quad K_1 = (\alpha^2 + \epsilon_o\Gamma)^{1/2}, \quad \epsilon_o = \frac{f^2}{gH^*k^2},$$
$$K_2 = (\alpha^2+\epsilon_o)^{1/2}, \qquad \tau = -\frac{f}{\sigma}.$$

Here G denotes the path from $\alpha = -\infty$ to $+\infty$ in the complex plane indented above the simple pole $\alpha = q$ on the real axis where $E(q) = 0$. For τ large, ϵ_o small, $q \simeq -\sqrt{\Gamma\epsilon_o}/\tau(\Gamma^{1/2} - 1)$. In (22) the first term is a standing wave response which decays as $|y| \longrightarrow \infty$. The last term represents a Double Kelvin wave type progressing in the negative y direction away from the wind disturbance which is concentrated about $y = 0$. Mysak calculates its asymptotic behavior only for $|y|$ large. Since the wavelengths are large and depth discontinuities in practice are of limited extent we have calculated the full response (22) for a wind force $\tau_o{}^x = 1$ dyne, $\Gamma = 1.3, f = 10^{-4}\,\text{sec}^{-1}$, $H^* = 4 \times 10^5$ cm, $g = 10^3$ cm sec^{-2}, $\sigma = 0.5 \times 10^{-5}$ sec^{-1}, $k = 1.58 \times 10^{-8}$ cm^{-1} so that $\epsilon_o = f^2/gH^*k^2 = 0.1$. The forcing period is about 15 days and the winds are mostly confined to a region of width 1500 km about $y = 0$. The free surface response is given in

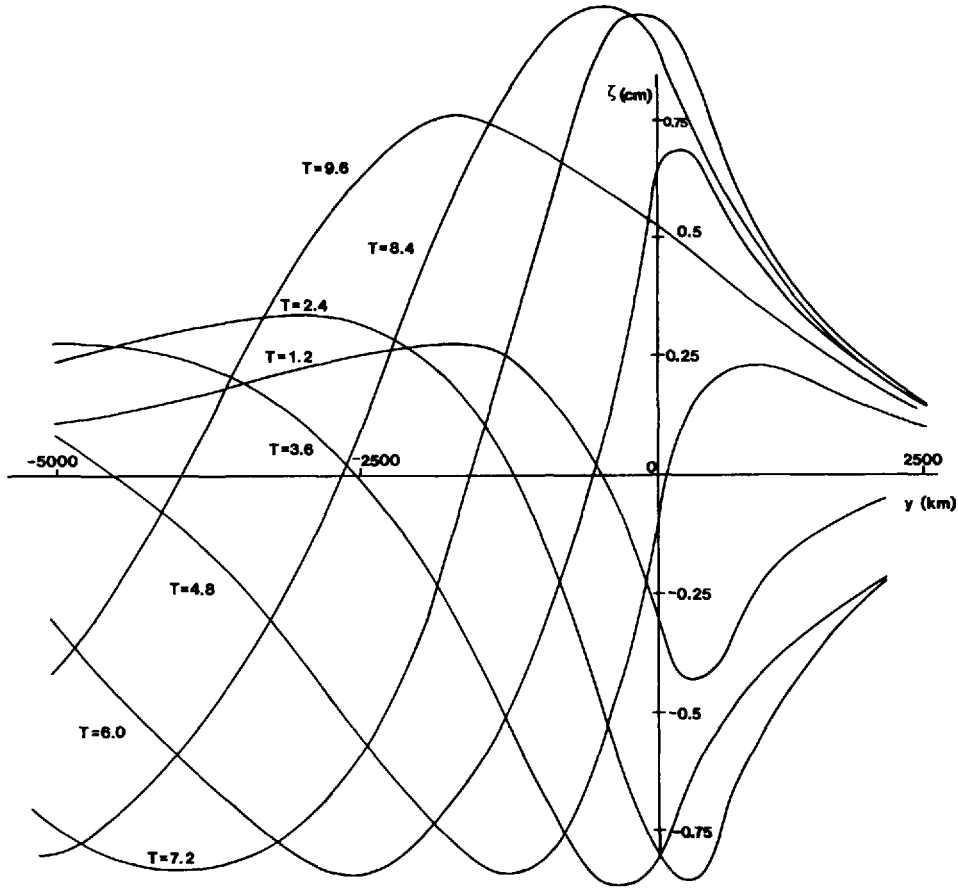

Figure 8. Free surface elevations at $x = 0$ plotted against y for a one-layer ocean at various times T measured in days due to a periodic wind stress given by (21) with $\tau_o^x = 1$ dyne, $H^* = 4 \times 10^5$ cm and forcing conditions $K = 1.58 \times 10^{-8}$ cm^{-1}, $\sigma = 0.5 \times 10^{-5}$ sec.

Figure 8. As can be seen as time increases (measured in the figure in days) there is a distinct movement away from the disturbance region in the negative y direction. These results are in accordance with those given by Mysak for slightly different conditions. We see that the elevations have a maximum amplitude of about 0.7 cm for a windstress $\tau_o^x = 1$ dyne. We discuss this case further below.

b. Two-layer case. For a two-layer case we adopt the same time period wind stress as given in (21). The theoretical response for free surface ζ and interface ζ' is very similar to (22), also consisting of a standing wave and a Double Kelvin type contribution. Since the equivalent expressions to (22) are quite complicated and long, only the numerical

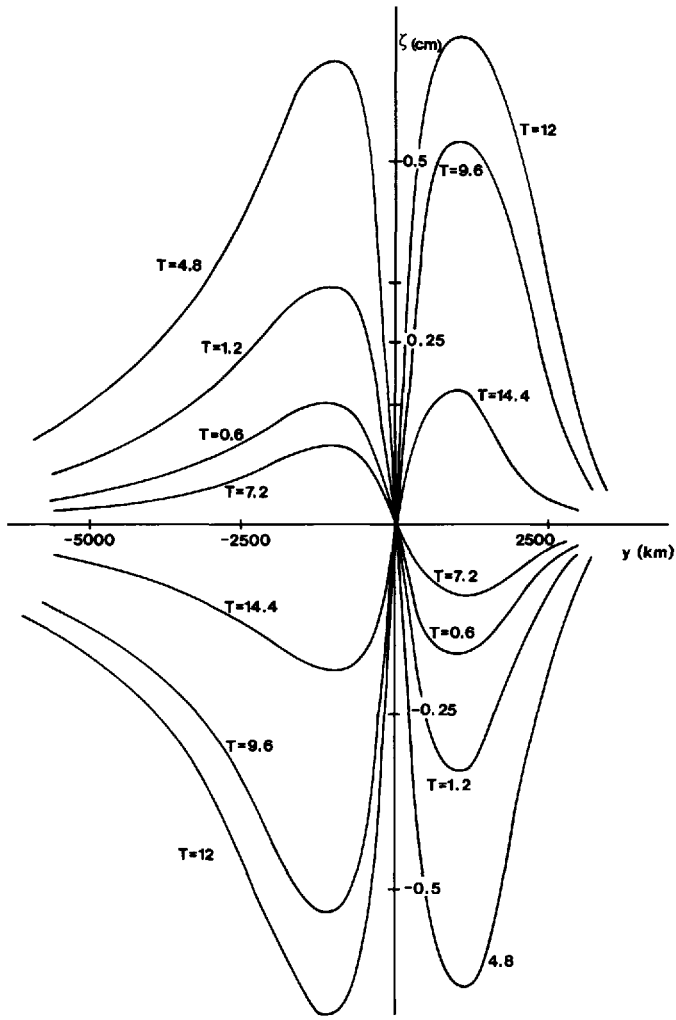

Figure 9. Free surface elevations of $x = 0$ against y for a two-layer ocean under the same wind stress and conditions as in Figure 8, for upper layer thickness $h = 4 \times 10^4$ cm^{-1} and $\rho/\rho' = .998$.

results are presented here in Figures 9, 10 for identical conditions as stated above in the case $\bar{h} = h/H = 0.1$. Full details are given by Bondok (1980).

The free surface response is shown in Figure 9. Although the elevations again have similar amplitudes to the one-layer case we see that the response appears to be dominated by the standing wave component. Only a relatively weak Double Kelvin type contribution is apparently present. The results for the interface elevation response given in Figure 10 on the other hand are similar in type to those of Figure 8. The

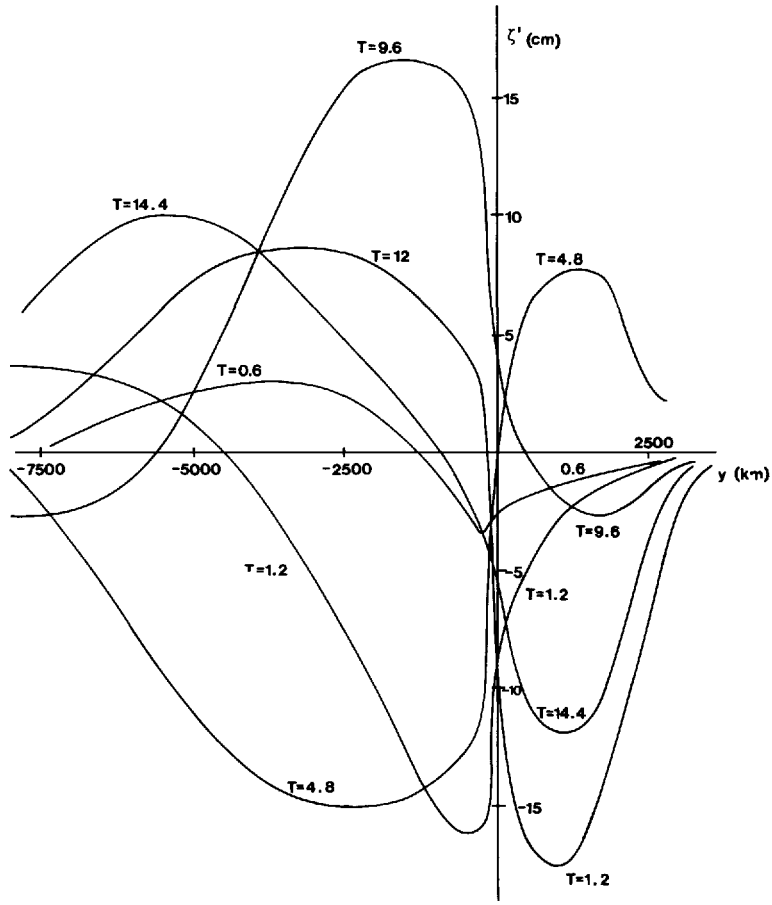

Figure 10. Interface elevation at $x = 0$ against y for a two-layer ocean under the same wind stress and conditions as in Figure 8, for upper layer thickness $h = 4 \times 10^4$ cm^{-1} and $\rho/\rho' = .998$.

interface maximum amplitudes are about 10–15 cm and there is a similar wave development moving in the $-y$ direction on a similar time scale as given in Figure 8. Although the Double Kelvin wave response in Figure 9 seems exceptional it must be remembered that our earlier work has indicated values of maximum elevation ratio R of about 70 as commonplace over step discontinuity. On this basis the expected free surface Double Kelvin wave amplitudes would be only of order 0.15 cm.

The periodic wind stress starting up at $t = 0$ has a forcing period of 20 pendulum days, or if $f = 10^{-4}$ sec^{-1}, 14.5 days. Figure 2 shows that over a depth discontinuity both the one-layer case and the two-layer case for $\bar{h} = h/H^* = 0.1$ have $\epsilon \simeq .37$. For $H^* = 4 \times 10^5$ cm this corresponds to a wavelength of Double Kelvin wave of about

7600 km, and a corresponding phase velocity of 22 km/hour. Looking in particular at Figures 8 and 10 for y large and negative, estimates of the period and wavelength of the wave motions seem to be in accordance with these results.

Mysak estimates maximum current velocities using typical free surface elevations of the Double Kelvin waves, generated by the wind stress, inserted into the equations of motion. Doing the same from Figure 8 we come to similar conclusions, i.e., the maximum current velocities in the one-layer case are of the order of 0.75 cm/sec for $\tau_o^x = 1$. For the two-layer case, Figure 9 reveals current velocities of the same order also occur in the upper layer but only for the standing waves which lie in the vicinity of the wind disturbance about $y = 0$. There is an absence of significant free surface elevations as y becomes large and negative, which in turn suggests much smaller current velocities occur in the upper layer for these Double Kelvin waves. In the lower layer the elevations given in Figure 10 appear to lead in this example to current velocities of the Double Kelvin waves also of about 0.75 cm/sec as for the one-layer ocean. The reason for this is that given the elevations in Figure 10 are large ($\simeq$10 cm) for y large and negative, and the transverse space derivatives of ζ' are also large, nevertheless ζ' in the equations occurs multiplied by a small factor $1 - \gamma = .002$. To conclude it would appear in this example that the upper layer in the two-layer ocean reacts to the wind stress only as a standing wave. The Double Kelvin wave moving away from the forcing zone takes the form of a submerged wave affecting only the lower layer. Although the current velocities in this lower layer are similar to those in the one-layer case through its whole depth, the interface elevations will be much larger. For a weather system of reasonable strength with $\tau_o^x = 3$ dynes these elevations are of order 30–40 cms. For this reason it may be possible to detect Double Kelvin waves in practice by looking at the thermocline.

REFERENCES

Bondok, S. A. W. 1980. Some effects of varying depth on trapped waves and ocean currents in one- and two-layer oceans. Ph.D. thesis, University of London.

Longuet-Higgins, M. S. 1968a. On the trapping of waves along a discontinuity of depth in a rotating ocean. J. Fluid Mech., *31,* 417–434.

—— 1968b. Double Kelvin waves with continuous depth profiles. J. Fluid Mech., *34,* 49–80.

Mysak, L. A. 1968. On the generation of Double Kelvin waves. J. Fluid Mech., *37,* 417–434.

Rhines, P. B. 1977. The dynamics of unsteady currents, *in* The Sea, E. Goldberg, ed., Wiley Interscience, New York, 189–318.

Received: *23 January, 1982;* revised: *29 July, 1983.*